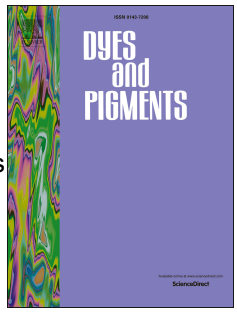

Synthesis and Photophysical Properties of Naphtho[*b*]- and Indeno[*b*]-fused BODIPYs

Baogeng Wu, Zhikuan Zhou, Lei Chen, Aihua Yuan

PII: S0143-7208(20)31373-5

DOI: https://doi.org/10.1016/j.dyepig.2020.108676

Reference: DYPI 108676

To appear in: *Dyes and Pigments*

Received Date: 30 May 2020

Revised Date: 27 June 2020

Accepted Date: 27 June 2020

Please cite this article as: Wu B, Zhou Z, Chen L, Yuan A, Synthesis and Photophysical Properties of Naphtho[*b*]- and Indeno[*b*]-fused BODIPYs, *Dyes and Pigments*, https://doi.org/10.1016/j.dyepig.2020.108676.

Baogeng Wu: Investigation, Formal analysis, Data curation. **Lei Chen:** Formal analysis. **Aihua Yuan:** Supervision, Writing - original draft. **Zhikuan Zhou:** Supervision, Writing - original draft, Writing - review & editing.

Synthesis and Photophysical Properties of Naphtho[*b*]- and Indeno[*b*]-fused BODIPYs

Baogeng Wu,[ab] Zhikuan Zhou,*[b] Lei Chen,[a] Aihua Yuan*[a]

a. School of Environmental and Chemical Engineering, Jiangsu University of Science and Technology, Zhenjiang 212003, China.

b. Key Laboratory of Organosilicon Chemistry and Material Technology of Ministry of Education, Key Laboratory of Organosilicon Material Technology of Zhejiang Province, Hangzhou Normal University, No. 2318, Yuhangtang Road, Hangzhou, 311121, China.

Corresponding Authors: zkzhou@hznu.edu.cn; aihua.yuan@just.edu.cn

Abstract

A new synthetic method to construct [*b*]-fused BODIPY derivatives through $PtCl_2$-catalyzed cycloisomerization reaction of peripherally phenylacetylene substituted BODIPYs is reported. Electron donating methoxy group facilitate both the 6-*endo* and 5-*exo* cyclization procedure to produce naphtho[*b*]- and indeno[*b*]-fused BODIPYs in one pot reaction. Naphtho[*b*]-fused BODIPY exhibits redshifted absorption and emission (591 nm/621 nm) with higher quantum yield (0.56 in DCM), while indeno[*b*]-fused BODIPY shows very low quantum yield (0.01 in DCM) with shorter absorption and emission wavelength (571 nm/600 nm) and stronger absorption intensity. Quantum-chemical calculation revealed the antiaromatic nature of cyclopentadienyl ring in indeno[*b*]-fused BODIPY, which accounts for its inferior photophyscal properties.

Keywords: BODIPY; [*b*]-fusion; photophysical properties; cyclization; TD-DFT calculation

1. Introduction

Due to the divers modification sites and excellent properties, 4-bora-3a,4a-diaza-s-indacene (BODIPY) dyes and their derivatives have attracted tremendous research interest in recent years.[1-4] BODIPYs possess rigid core

structure and conjugated π systems, which can be further extended through phostfunctionalization to meet wider applications.[4-6] π-extended BODIPYs with near-infrared (NIR) absorbtion and emission are promising to be utilized for bioimaging,[3, 7-12] photodynamic therapy (PDT),[13-25] organic field electron transfer (OFET) materials,[26, 27] and other advanced electronic and optical materials.[28-32]

Various π-extended BODIPYs have been synthesized through substitution or ring fusion of aromatic groups at peripheral positions, and construction of conjugated oligomers.[33-39] Among them, aromatic ring-fused BODIPYs are particularly promising with extension of rigid π skeleton and excellent electronic properties. Depending on the position on which the aromatic ring fused, annulated BODIPYs can be classified into [*a*]-,[40, 41] [*b*]-,[35, 42, 43] zig-zag-,[44, 45] and boron-fused[46] patterns. The [*b*]-fusion could effectively decrease the LUMO level, which is prone to obtain air stable NIR dyes.[47] To achieve annulated BODIPYs, postfunctionalization of BODIPY core is more versatile than the *de novo* synthesis utilizing aromatic ring-fused pyrroles as starting materials, which are difficult to obtain and easy to be oxidized under ambient condition.[48, 49] The key procedure for postfunctionalization is to rationally preinstall the aromatic ring on the proper peripheral site of BODIPY core for further annulation. Acid-induced intramolecular cyclization are commonly employed for the efficient fabrication of aromatic ring [*b*]-fused BODIPYs.[26, 42, 50, 51] However, in some cases, strong acid could lead to spontaneous deboronation of BODIPY core structures, which made the direct annulation reaction frustrated.[52, 53] As alternative, transition metal catalyzed C-H functionalization seems to be an easy-to-operate way to rationally control the fusion mode of aromatic rings.[40, 54, 55]

Dienylalkyne derivatives are versatile building blocks for the synthesis of carbo and hetero polycyclic aromatics.[56-58] With the assistance of acid, base, or metal-based catalyst, straightforward 6-endo or 5-exo cyclization may occur, which results in the formation of benzo[*b*]- or methylenecyclopenta[*b*]-fused derivatives (**Scheme 1**). $PtCl_2$ has been widely used as catalyst for carbocyclization of

alkynylated biaryl derivatives to fabricate aromatic fused molecules.[59, 60] In the BODIPY precursor **A**, through the rational substitution at the β-position of pyrrole unit, an intramolecular dienylalkyne structure is fabricated, which should be prone to cyclize under $PtCl_2$ catalyzation to produce two possible isomers. In pursuit of aromatic ring [*b*]-fused BODIPY, and based on our previous investigations,[43, 61] we now report the synthesis and photophysical properties of mono-naphtho[*b*]-fused and indeno[*b*]-fused BODIPYs via $PdCl_2$-catalysed intramolecular cycloisomerization reaction.

2. Results and Discussion

2.1. Synthesis

1-bromo-2-(4-R-phenylethynyl)benzene **1a-1c** were synthesized through Sonogashira cross-coupling of substituted iodobenzene with substituted phenylacetylene in the yield of 70% to 76% (See details in Supplementary data). Borate compounds **2a**-**2c** were synthesized through the substitution of bromine atom by pinacolatoboron (Bpin) group, which was carried out by lithium halogen exchange reaction and subsequent reaction with 2-isopropoxy-4,4,5,5-tetramethyl-1,3,2-dioxaborolane in the yield of 73% to 86%. Standard Suzuki-Miyaura cross-coupling reactions employing **2** and 2-bromo BODIPY **6**[62] afford the key BODIPY precursors **3**. The final intramolecular cycloaromatization procedure was conducted under the catalyzing of $PtCl_2$ without any extra adducts in reflux toluene for 12 h. Lower reaction temperature results in lower yield, while longer reaction time did not improve the yield but lead to the decomposition of the target compounds. Interestingly, it was found that the major ring-fused products varied according to the substitution on the para position of phenylacetylene. Electron-donating methoxy group facilitated the formation of both 6-endo and 5-exo products, namely naphtho[*b*]-fused BODIPY **4b** and indeno[*b*]-fused BODIPY **5b**, respectively (**Scheme 2**). Phenyl and electron-withdrawing trifluoromethyl groups substituted precursors prompted the

6-endo reaction against the 5-exo pathway. The same substituent effect has been reported in $PtCl_2$-catalyzed cycloisomerization reactions for phenanthrenes.[59, 60] The aromatic ring fused BODIPYs **4a**, **4b**, **4c**, and **5b** were characterized by high-resolution mass spectroscopy (HR-MS) and NMR spectroscopy. HR-ESI-MS showed the peaks of the molecular ion $[M + Na]^+$ at *m/z* = 539.2070 and *m/z* = 539.2080 for **4b** and **5b**, respectively, clarifying that they are isomeric compounds.

In principle, the cycloaromatization reaction of BODIPY **3** could occur between alkynyl group and the adjacent α or γ position of pyrrole unit to give either [*a*]- or [*b*]-fused species. The ^{1}H NMR spectra of **4b** and **5b** clearly showed the absence of the singlet peak of α proton of BODIPY **3b** at 8.59 ppm,[51] while the γ proton still exist after the cycloaromatization reaction at 7.40 and 7.31 ppm, respectively (**Fig. 1**). The major structural difference between **4b** and **5b** is the position of ω protons. In naphtho[*b*]-fused BODIPY **4b**, the ω proton is fixed on the phenyl group in the aromatic BODIPY skeleton, thus it appears at lower field (8.03 ppm) due to the lower electronic density on the neighboring carbon.[43] While in indeno[*b*]-fused BODIPY **5b**, the ω proton is located on a typical vinyl group, it appears at upper field (7.53 ppm).[63]

2.2. X-ray single crystal structures

Single crystals of **3b** and **3c** were obtained from the slow evaporation of n-hexane into their dichloromethane solutions at room temperature. The diphenylacetylene fragment rotate around the 2-position of BODIPY core with the OCH_3 and CF_3 "tail" oriented upward to the meso-mesityl group (**Fig. 2**). In **3b** and **3c**, the dihedral angles between phenyl group **A** and BODIPY core **C** are 18.6^o and 34.5^o, respectively. The dihedral angels between phenyl rings **A** and **B** in **3b** and **3c** are 13.5^o and 17.7^o, respectively. These results indicated the twisted conformation and the existence of considerable repulsion between the diphenylacetylene unit and BODIPY core, which suggested the difficulty of intramolecular cyclization in the [*a*]-fused fashion.

2.3. Photophysical properties

The absorption and emission spectra of the aromatic ring fused BODIPYs **4a**-**4c**, and **5b** in CH_2Cl_2 are shown in **Fig. 3** and the photophysical properties are summarized in **Table 1**. The absorption and fluorescence emission spectra in n-hexane, toluene, THF, and acetonitrile are plotted in **Fig. S1-S7**, the detailed photophysical data are summarized in **Table S1**. The precursor BODIPYs **3a**-**3c** exhibit large stocks shifts ranging from 50 nm to 56 nm with quantum yield around 0.2. Upon cyclization to form [*b*]-fused BODIPYs **4a**-**4c**, and **5b**, the absorption maxima redshifted 31 nm to 53 nm, indicating the efficient extension of π systems. The observed absorption and emission band maxima of the same compound fluctuated within 23 nm in different solvents. However, no obvious trend as function of polarity of the solvent was found (**Fig. S4-S7**). Different from BODIPYs **4a**-**4c**, the molar extinction coefficient and emission intensity of BODIPY **5b** differed largely in various solvents, indicating the unique photophysical properties brought by its indeno[*b*]-fused structure. For naphtho[*b*]-fused BODIPY **4a**-**4c**, it is interesting that **4b** absorb and emit at longer wavelength than both **4a** and **4c** with quantum yield of 3 times higher than the later ones. It can be deduced that the methoxy group on the unfused phenyl unit at BODIPY 3 position aid in the extention of π system. The indeno[*b*]-fused BODIPY **5b** exhibits almost the same absorption and emission band maxima as **4a** and **4c**, while the molar absorption coefficient increased nearly 2 times (91000 $M^{-1}cm^{-1}$). The indeno[*b*]-fusion mode leads to dramatic decrease of fluorescence quantum yield of **5a** (0.01 in DCM).

2.4. TD-DFT calculation

DFT calculations with B3LYP functional and 6-31G(d) basis set were carried out to get depth insight into the structure-spectroscopy relationship. The optimized conformation of **3b** and **3c** were the same with their crystal structures. In principle, *cis*- and *trans*- isomers of BODIPY **5b** may be generated during the formation of vinyl compound. The comparison of the electronic energy of these two isomers revealed that the *cis*-isomer shown in **Fig. 4** is more stable (**Fig. S8**), which is chosen to be studied in the following part. The 6-*endo* fusion compounds **4a** and **4c** possessed

more stabilized LUMO and destabilized HOMO energy compared with their precursors **3a** and **3c** (**Fig. S9** and **Fig. S11**), which consequently decreased their HOMO-LUMO gaps and resulted in the redshifted absorption. When compared with **3b**, the 6-*endo* fusion only stabilized the LUMO energy of **4b**, while the 5-*exo* fusion destabilized both the HOMO and LUMO energies of **5b**. As a result, the HOMO-LUMO gaps of **4b** was smaller than that of **5b**, which corresponded with the observed red-shifts in the absorption maxima of **4b**. When carefully check the frontier MOs of **4b** and **5b**, it is clearly to observe that the electron density on their HOMO spread all over the BODIPY core, fused phenyl and methoxyphenyl group. However, the electron density on the LUMO of **5b** not only located on the BODIPY core and fused phenyl, but also spread over the methoxyphenyl group, which differed from **4b** and largely destabilized the LUMO of **5b**. We could conclude that the methoxy group aid in the delocalization of electron density over the cycloarmatization products.

To better understand the origin of difference in UV-Vis spectra of isomers **4b** and **5b**, TD-DFT calculations were performed for them and the results were plotted and summarized in **Fig. 5** and **Table S2**. The calculated maximum absorption peaks of both **4b** and **5b** mainly composed of HOMO to LUMO transition and HOMO-1 to LUMO transition. The calculated absorption maxima of **4b** is larger than **5b**, but the oscillator strength is much smaller, which is in accordance with the experimental data. The nucleus-independent chemical shift (NICS)(0) values of selected five or six-membered rings were calculated to examine their aromaticity (**Fig. 5**). NICS(0) values of the selected pyrrole ring in BODIPYs **4b** and **5b** were -7.66 and -4.53 ppm, respectively, indicating the more aromatic nature of the BODIPY core of **4b**.[42] This is mainly affected by the character of [*b*] fused rings. The fused phenyl ring in **4b** still retain the aromatic nature with a NICS(0) value of -4.47 ppm, however, the fused cyclopentadienyl ring in **5b** became antiaromatic with a NICS(0) value of 2.69 ppm, which is totally different from the analogous five-membered heterocycles such as thiophene.[27, 53] Thus, the global aromaticity of **5b** is weakened, which also have inferior extension of π-conjugation after ring fusion.

3. Conclusion

In summary, we have synthesized a series of aromatic ring [*b*]-fused BODIPYs through $PtCl_2$-catalyzed intramolecular cycloisomerization reaction between peripherally preinstalled alkynyl group and pyrrole unit of BODIPY core. No substituent or electron withdrawing CF_3 on the para position of phenylethynyl group result in the exclusive formation of 6-*endo* product, while electron donation methoxy group facilitate the formation of both 6-*endo* and 5-*exo* products in one pot. The photophysical properties of all the aromatic ring [*b*]-fused BODIPYs were investigated. Naphtho[*b*]-fused BODIPY with methoxy substitution exhibits the most redshifted absorption and emission (591 nm/621 nm) and the highest quantum yield (0.56 in DCM), while indeno[*b*]-fused BODIPY shows the lowest quantum yield (0.01 in DCM) with shorter absorption and emission wavelength (571 nm/600 nm) and the strongest absorption intensity (91000 $M^{-1}cm^{-1}$). Quantum calculation revealed the aromatic nature of the [*b*]-fused phenyl ring in naphtho[*b*]-fused BODIPY, on the contrary, the fused cyclopentadienyl ring in indeno[*b*]-fused BODIPY exhibited antiaromatic character, which accounts for the dramatic difference in their photophysical properties.

4. Materials and methods

4.1 Instruments and reagents

All reagents were obtained from commercial suppliers and used without further purification unless otherwise indicated. All air and moisture-sensitive reactions were carried out under nitrogen atmosphere in oven-dried glassware. Glassware was dried in an oven at 100°C and cooled under a stream of inert gas before use. Both dichloromethane and triethylamine were distilled over calcium hydride before use. ^{1}H-NMR spectra were recorded on a Bruker DRX400 spectrometer and referenced to the residual proton signals of the solvent. HR-MS were recorded on a Bruker Daltonics microTOF-Q II spectrometer. All the solvents employed for the spectroscopic measurements were of UV spectroscopic grade (Aldrich).

4.2. Synthesis

*4.2.1 Synthesis of compound **1**, **2**, and BODIPY **6***

The detailed synthetic procedures of **1** and **2** were summarized in the supplementary data. 2-Bromo-BODIPY **6** was synthesized according to the literature [62].

*4.2.2 Synthesis of **3a**, **3b**, and **3c***

A solution of BODIPY-Br **6** (380 mg, 1 mmol), **2a** (335 mg, 1.1 mmol) in THF (20 mL) were added into 100 mL flask filled with nitrogen. $Pd(PPh_3)_4$ (116 mg, 0.1 mmol) was added under nitrogen, then 3 mL 2 mol/L Na_2CO_3 was added. The reaction was heated to reflux for 4 h. The reaction was monitored by TLC. After completion, the solvent was removed and the residue was purified by silica gel column chromatography eluting with 20% to 40% dichloromethane / petroleum ether. Red solid, 400 mg, yield 83 %. ^{1}H NMR (400 MHz, $CDCl_3$) δ 8.55 (s, 1H), 7.93 (s, 1H), 7.62 – 7.56 (m, 1H), 7.47 (d, *J* = 7.7 Hz, 1H), 7.38 (dd, *J* = 7.1, 2.7 Hz, 2H), 7.33 (dd, *J* = 6.5, 1.6 Hz, 4H), 7.27 (s, 1H), 7.23 (d, *J* = 3.7 Hz, 1H), 6.91 (s, 2H), 6.68 (d, *J* = 4.0 Hz, 1H), 6.48 (d, *J* = 2.7 Hz, 1H), 2.36 (s, 3H), 2.11 (s, 6H). ^{13}C NMR (100 MHz, $CDCl_3$) δ 144.38, 144.18, 138.76, 136.37, 134.14, 133.80, 131.43, 130.02, 129.68, 128.70, 128.34, 127.58, 127.29, 122.92, 120.43, 93.68, 89.19, 21.20, 20.11 ppm. HRMS-ESI: *m/z*: calcd. for $[C_{32}H_{25}BF_2N_2+Na]^+$:509.1977, found:509.1966.

The synthesis of compounds **3b** and **3c** were obtained by following a similar procedure to that of **3a**.

Compound **3b** was obtained in 58% yield as red solid. ^{1}H NMR (400 MHz, $CDCl_3$) δ 8.59 (s, 1H), 7.93 (s, 1H), 7.56 (d, *J* = 8.6 Hz, 1H), 7.45 (d, *J* = 7.6 Hz, 1H), 7.34 (s, 1H), 7.32 (s, 1H), 7.28 (d, *J* = 9.0 Hz, 1H), 7.22 (d, *J* = 15.4 Hz, 2H), 6.93 (s, 2H), 6.87 (d, *J* = 8.8 Hz, 2H), 6.68 (d, *J* = 4.0 Hz, 1H), 6.48 (d, *J* = 3.9 Hz, 1H), 3.85 (s, 3H), 2.37 (s, 3H), 2.12 (s, 6H). ^{13}C NMR (100 MHz, $CDCl_3$) δ:159.87, 138.86, 136.51, 133.95, 133.66, 133.03, 129.82, 128.44, 128.36, 127.66, 127.33, 93.98, 88.12, 55.46, 21.34, 20.26 ppm. HRMS-ESI: *m/z*: calcd. for $[C_{32}H_{25}BF_2N_2+Na]^+$: 539.2082, found: 539.2085.

Compound **3c** was obtained in 69% yield as red solid. ^{1}H NMR (400 MHz,

$CDCl_3$) δ 8.54 (s, 1H), 7.95 (s, 1H), 7.60 (d, *J* = 8.6 Hz, 3H), 7.49 (d, *J* = 7.9 Hz, 3H), 7.36 (td, *J* = 7.7, 1.4 Hz, 1H), 7.29 – 7.27 (m, 1H), 7.17 (s, 1H), 6.91 (s, 2H), 6.70 (d, *J* = 4.1 Hz, 1H), 6.52 – 6.48 (m, 1H), 2.35 (s, 3H), 2.12 (s, 6H). ^{13}C NMR (100 MHz, $CDCl_3$) δ 144.62, 143.99, 136.35, 133.84, 131.62, 130.35, 129.29, 128.27, 127.69, 127.18, 125.28, 21.11, 20.12 ppm. HRMS-ESI: *m/z*: calcd. for $[C_{33}H_{24}BF_5N_2+Na]^+$: 577.1851, found: 577.1840.

*4.2.3 Synthesis of **4a** and **4c***

3a (200 mg, 0.41 mmol) was added into 100 mL flask filled with nitrogen. Dry toluene (10 mL) was added. $PtCl_2$ (15 mg, 0.05 mmol) was then added under nitrogen. The mixture was heated under 110 □ overnight before cooled to room temperature. The solvent was removed and the residue was purified by silica gel column chromatography eluting with 40% dichloromethane / petroleum ether. **4a**, Black solid, 50 mg, yield 25 %. ^{1}H NMR (400 MHz, $CDCl_3$) δ 8.03 (d, *J* = 7.8 Hz, 1H), 7.88 (s, 1H), 7.73 (d, *J* = 7.6 Hz, 1H), 7.59 (d, *J* = 3.0 Hz, 2H), 7.55 (s, 1H), 7.52 – 7.46 (m, 4H), 7.46 – 7.42 (m, 1H), 7.41 (s, 1H), 7.03 (s, 2H), 6.72 (d, *J* = 4.2 Hz, 1H), 6.49 (d, *J* = 3.1 Hz, 1H), 2.43 (s, 3H), 2.16 (s, 6H). ^{13}C NMR (100 MHz, $CDCl_3$) δ 146.35, 135.75, 135.07, 130.73, 129.30, 128.20, 127.81, 127.23, 126.91, 126.46, 125.97, 124.96, 122.17, 120.37, 28.68, 19.15 ppm. Elemental analysis calcd. (%) for $C_{32}H_{25}BF_2N_2$: C 79.02, H 5.18, N 5.76. Found: C 79.37, H 4.95, N 5.44. HRMS-ESI: *m/z*: calcd. for $[C_{32}H_{25}BF_2N_2+Na]^+$: 509.1977, found: 509.1966.

The synthesis of BODIPY **4c** were obtained by following a similar procedure to that of **4a**.

Compound **4c** was obtained in 40% yield as black solid. ^{1}H NMR (400 MHz, $CDCl_3$) δ 8.04 (d, *J* = 7.9 Hz, 1H), 7.86 (s, 1H), 7.74 (dd, *J* = 8.1, 4.1 Hz, 3H), 7.69 (d, *J* = 8.2 Hz, 2H), 7.55 – 7.48 (m, 2H), 7.46 (d, *J* = 8.0 Hz, 1H), 7.41 (s, 1H), 7.04 (s, 2H), 6.75 (d, *J* = 4.2 Hz, 1H), 6.52 (d, *J* = 3.2 Hz, 1H), 2.43 (s, 3H), 2.16 (s, 6H). ^{13}C NMR (100 MHz, $CDCl_3$) δ 147.78, 139.14, 136.75, 135.74, 131.62, 130.82, 130.35, 130.11, 129.30, 129.02, 128.95, 128.32, 128.27, 128.11, 127.89, 126.12, 124.04, 123.26, 121.15, 21.24, 20.19, 20.12 ppm. Elemental analysis calcd. (%) for

$C_{33}H_{24}BF_5N_2$: C 71.50, H 4.36, N 5.05. Found: C 71.72, H 4.67, N 5.39. HRMS-ESI: *m/z*: calcd. for $[C_{33}H_{24}BF_5N_2+Na]^+$: 577.1851, found: 577.1840.

*4.2.4 Synthesis of **4b** and **5b***

3b (200 mg, 0.38 mmol) was added into 100 mL flask filled with nitrogen. Dry toluene (10 mL) was added. Then, $PtCl_2$ (15 mg, 0.05 mmol) was added under nitrogen. The mixture was heated under 110 □ overnight before cooled to room temperature. The solvent was removed and the residue was purified by silica gel column chromatography eluting with 40% dichloromethane / petroleum ether. Black solid **4b**, 30 mg, yield 20%; Black solid **5b**, 50 mg, yield 25%.

4b ^{1}H NMR (400 MHz, $CDCl_3$) δ 8.04 (d, *J* = 7.3 Hz, 2H), 7.84 (d, *J* = 7.9 Hz, 1H), 7.77 (s, 1H), 7.49 (d, *J* = 8.6 Hz, 3H), 7.37 (s, 1H), 7.31 (s, 1H), 7.07 – 7.01 (m, 4H), 6.75 (d, *J* = 4.1 Hz, 1H), 6.56 (dd, *J* = 4.3, 1.7 Hz, 1H), 3.91 (s, 3H), 2.43 (s, 3H), 2.17 (s, 6H). ^{13}C NMR (100 MHz, $CDCl_3$) δ 167.73, 159.56, 151.54, 146.51, 145.69, 139.02, 135.77, 132.39, 130.09,129.05, 128.87, 127.71, 125.84, 124.92, 123.99, 120.87, 119.88, 116.58, 113.81, 55.44, 34.25, 30.34, 20.20, 14,17 ppm. Elemental analysis calcd. (%) for $C_{33}H_{27}BF_2N_2O$: C 76.76, H 5.27, N 5.42, O 3.10. Found: C 76.54, H 5.03, N 5.27. HRMS-ESI: *m/z*: calcd. for $[C_{33}H_{27}BF_2N_2O+Na]^+$: 539.2082, found: 539.2070.

5b ^{1}H NMR (400 MHz, $CDCl_3$) δ 8.02 (d, *J* = 7.9 Hz, 1H), 7.88 (s, 1H), 7.72 (d, *J* = 7.7 Hz, 1H), 7.50 (dd, *J* = 17.9, 10.0 Hz, 4H), 7.45 – 7.37 (m, 2H), 7.02 (d, *J* = 6.5 Hz, 4H), 6.72 (d, *J* = 3.6 Hz, 1H), 6.49 (d, *J* = 3.3 Hz, 1H), 3.92 (s, 3H), 2.43 (s, 3H), 2.15 (s, 6H). ^{13}C NMR (100 MHz, $CDCl_3$) δ 159.06, 147.35, 139.12, 136.90, 136.67, 131.58, 130.63, 130.39, 129.45, 128.92, 128.38, 128.02, 127.63, 126.10, 123.31, 121.57, 120.84, 112.52, 55.33, 21.37, 20.32 ppm. Elemental analysis calcd. (%) for $C_{33}H_{27}BF_2N_2O$: C 76.76, H 5.27, N 5.42, O 3.10. Found: C 76.49, H 5.46, N 5.30. HRMS-ESI: *m/z*: calcd. for $[C_{33}H_{27}BF_2N_2O+Na]^+$: 539.2082, found: 539.2070.

Conflicts of interest

There are no conflicts to declare.

Acknowledgements

We thank the National Natural Science Foundation of China (No. 21501073), the organosilicon chemistry innovation team, the research funding project of Hangzhou Normal University (2019QDL019) for financial support. Theoretical calculations were carried out at the Computational Centre for Molecular Design of Organosilicon Compounds, Hangzhou Normal University.

Reference

[1] Boens N, Verbelen B, Ortiz MJ, Jiao L, Dehaen W. Synthesis of BODIPY dyes through postfunctionalization of the boron dipyrromethene core. *Coord Chem Rev,* 2019:399:213024.

[2] Boodts S, Fron E, Hofkens J, Dehaen W. The BOPHY fluorophore with double boron chelation: Synthesis and spectroscopy. *Coord Chem Rev,* 2018:371:1-10.

[3] Kowada T, Maeda H, Kikuchi K. BODIPY-based probes for the fluorescence imaging of biomolecules in living cells. *Chem Soc Rev,* 2015:44(14):4953-4972.

[4] Lu H, Mack J, Yang Y, Shen Z. Structural modification strategies for the rational design of red/NIR region BODIPYs. *Chem Soc Rev,* 2014:43(13):4778-4823.

[5] Zheng X, Du W, Gai L, Xiao X, Li Z, Xu L, et al. Disilanylene-bridged BODIPY-based D–σ–A architectures: a novel promising series of NLO chromophores. *Chem Commun,* 2018:54(64):8834-8837.

[6] Wu Y, Mack J, Xiao X, Li Z, Shen Z, Lu H. N-Bridged Annulated BODIPYs: Synthesis of Highly Fluorescent Blueshifted Dyes. *Chem - Asian J,* 2017:12(17):2216-2220.

[7] Shirbhate ME, Kwon S, Song A, Kim S, Kim D, Huang H, et al. Optical and Fluorescent Dual Sensing of Aminoalcohols by in Situ Generation of BODIPY-like Chromophore. *J Am Chem Soc,* 2020:142(11):4975-4979.

[8] Yang J, Fan Y, Cai F, Xu X, Fu B, Wang S, et al. BODIPY derivatives bearing borneol moieties: Enhancing cell membrane permeability for living cell imaging. *Dyes Pigments,* 2019:164:105-111.

[9] Kong X, Di L, Fan Y, Zhou Z, Feng X, Gai L, et al. Lysosome-targeting turn-on red/NIR BODIPY probes for imaging hypoxic cells. *Chem Commun,* 2019:55(77):11567-11570.

[10] Wu H, Guo X, Yu C, Wong W-Y, Hao E, Jiao L. Highly photostable ketopyrrolyl-BODIPYs with red aggregation-induced emission characteristics for ultrafast wash-free mitochondria-targeted bioimaging. *Dyes Pigments,* 2020:176:108209.

[11] Zhang Y, Zheng X, Zhang L, Yang Z, Chen L, Wang L, et al. Red fluorescent pyrazoline-BODIPY nanoparticles for ultrafast and long-term bioimaging. *Org Biomol Chem,* 2020:18(4):707-714.

[12] Sedgwick AC, Chapman RSL, Gardiner JE, Peacock LR, Kim G, Yoon J, et al. A bodipy based hydroxylamine sensor. *Chem Commun,* 2017:53(75):10441-10443.

[13] Nguyen V-N, Yim Y, Kim S, Ryu B, Swamy KMK, Kim G, et al. Molecular Design of Highly Efficient Heavy-Atom-Free Triplet BODIPY Derivatives for Photodynamic Therapy and Bioimaging. *Angew Chem Int Ed,* 2020:59(23):8957-8962.

[14] Zhang Y, Yang Z, Zheng X, Yang L, Song N, Zhang L, et al. Heavy atom substituted near-infrared BODIPY nanoparticles for photodynamic therapy. *Dyes Pigments*, 2020:178:108348.

[15] Zhang Y, Song N, Li Y, Yang Z, Chen L, Sun T, et al. Comparative study of two near-infrared coumarin–BODIPY dyes for bioimaging and photothermal therapy of cancer. *Journal of Materials Chemistry B*, 2019:7(30):4717-4724.

[16] Qu X, Song W, Shen Z. A Highly Selective NIR Fluorescent Turn-on Probe for Hydroxyl Radical and Its Application in Living Cell Images. *Front Chem*, 2019:7(598).

[17] Song N, Fu L, Liu Y, Li Y, Chen L, Wang X, et al. Rational design of BODIPY organic nanoparticles for enhanced photodynamic/photothermal therapy. *Dyes Pigments*, 2019:162:295-302.

[18] Su Y, Lu S, Gao P, Zheng M, Xie Z. BODIPY@carbon dot nanocomposites for enhanced photodynamic activity. *Mater Chem Front*, 2019:3(9):1747-1753.

[19] Li Z, Liu Y, Hou X, Xu Z, Liu C, Zhang F, et al. The crystal structures, spectrometric, photodynamic properties and bioimaging of β-β linked Bodipy oligomers. *J Lumin*, 2019:212:306-314.

[20] Ruan Z, Miao W, Yuan P, Le L, Jiao L, Hao E, et al. High Singlet Oxygen Yield Photosensitizer Based Polypeptide Nanoparticles for Low-Power Near-Infrared Light Imaging-Guided Photodynamic Therapy. *Bioconjugate Chem*, 2018:29(10):3441-3451.

[21] Li X, Kolemen S, Yoon J, Akkaya EU. Activatable Photosensitizers: Agents for Selective Photodynamic Therapy. *Adv Funct Mater*, 2017:27(5):1604053.

[22] Huang L, Zhao Y, Zhang H, Huang K, Yang J, Han G. Expanding Anti-Stokes Shifting in Triplet–Triplet Annihilation Upconversion for In Vivo Anticancer Prodrug Activation. *Angew Chem Int Ed*, 2017:56(46):14400-14404.

[23] Huang L, Li Z, Zhao Y, Zhang Y, Wu S, Zhao J, et al. Ultralow-Power Near Infrared Lamp Light Operable Targeted Organic Nanoparticle Photodynamic Therapy. *J Am Chem Soc*, 2016:138(44):14586-14591.

[24] Yang Y, Guo Q, Chen H, Zhou Z, Guo Z, Shen Z. Thienopyrrole-expanded BODIPY as a potential NIR photosensitizer for photodynamic therapy. *Chem Commun*, 2013:49(38):3940-3942.

[25] Kamkaew A, Lim SH, Lee HB, Kiew LV, Chung LY, Burgess K. BODIPY dyes in photodynamic therapy. *Chem Soc Rev*, 2013:42(1):77-88.

[26] Sheng W, Zheng Y-Q, Wu Q, Wu Y, Yu C, Jiao L, et al. Synthesis, Properties, and Semiconducting Characteristics of BF2 Complexes of β,β-Bisphenanthrene-Fused Azadipyrromethenes. *Org Lett*, 2017:19(11):2893-2896.

[27] Sheng W, Chang F, Wu Q, Hao E, Jiao L, Wang J-Y, et al. Synthesis and Semiconducting Characteristics of the BF2 Complexes of Bisbenzothiophene-Fused Azadipyrromethenes. *Org Lett*, 2020:22(1):185-189.

[28] Yang J, Devillers CH, Fleurat-Lessard P, Jiang H, Wang S, Gros CP, et al. Carbazole-based green and blue-BODIPY dyads and triads as donors for bulk heterojunction organic solar cells. *Dalton Trans*, 2020:49(17):5606-5617.

[29] Yi G, Zhang C, Zhao W, Cui H, Chen L, Wang Z, et al. Structure, magnetic anisotropy and relaxation behavior of seven-coordinate Co(ii) single-ion magnets perturbed by counter-anions. *Dalton Trans*, 2020:DOI: 10.1039/d1030dt01232g.

[30] Li Q, Shi C, Huang M, Wei X, Yan H, Yang C, et al. B- and N-embedded color-tunable

phosphorescent iridium complexes and B–N Lewis adducts with intriguing structural and optical changes. *Chem Sci*, 2019:10(11):3257-3263.

[31] Yu C, Huang Z, Gu W, Wu Q, Hao E, Xiao Y, et al. A novel family of AIE-active meso-2-ketopyrrolyl BODIPYs: bright solid-state red fluorescence, morphological properties and application as viscosimeters in live cells. *Mater Chem Front*, 2019:3(9):1823-1832.

[32] Yi G, Cui H, Zhang C, Zhao W, Chen L, Zhang Y-Q, et al. A capped trigonal prismatic cobalt(ii) complex as a structural archetype for single-ion magnets. *Dalton Trans*, 2020:49(7):2063-2067.

[33] Xu X, Sun D, Yang J, Zhu G, Fang Y, Gros CP, et al. Truxene-BODIPY dyads and triads: Synthesis, spectroscopic characterization, one and two-photon absorption properties and electrochemistry. *Dyes Pigments*, 2020:179:108380.

[34] Tao J, Sun D, Sun L, Li Z, Fu B, Liu J, et al. Tuning the photo-physical properties of BODIPY dyes: Effects of 1, 3, 5, 7- substitution on their optical and electrochemical behaviours. *Dyes Pigments*, 2019:168:166-174.

[35] Sun Y, Qu Z, Zhou Z, Gai L, Lu H. Thieno[3,2-b]thiophene fused BODIPYs: synthesis, near-infrared luminescence and photosensitive properties. *Org Biomol Chem*, 2019:17(14):3617-3622.

[36] Sun Y, Yuan H, Di L, Zhou Z, Gai L, Xiao X, et al. Non-symmetric thieno[3,2-b]thiophene-fused BODIPYs: synthesis, spectroscopic properties and providing a functional strategy for NIR probes. *Org Chem Front*, 2019:6(24):3961-3968.

[37] Huaulmé Q, Fall S, Lévêque P, Ulrich G, Leclerc N. Pairing of α-Fused BODIPY: Towards Panchromatic n-Type Semiconducting Materials. *Chem - Eur J*, 2019:25(26):6613-6620.

[38] Bura T, Retailleau P, Ulrich G, Ziessel R. Highly Substituted Bodipy Dyes with Spectroscopic Features Sensitive to the Environment. *J Org Chem*, 2011:76(4):1109-1117.

[39] Buyukcakir O, Bozdemir OA, Kolemen S, Erbas S, Akkaya EU. Tetrastyryl-Bodipy Dyes: Convenient Synthesis and Characterization of Elusive Near IR Fluorophores. *Org Lett*, 2009:11(20):4644-4647.

[40] Sheng W, Cui J, Ruan Z, Yan L, Wu Q, Yu C, et al. [a]-Phenanthrene-Fused BF2 Azadipyrromethene (AzaBODIPY) Dyes as Bright Near-Infrared Fluorophores. *J Org Chem*, 2017:82(19):10341-10349.

[41] Shen Z, Röhr H, Rurack K, Uno H, Spieles M, Schulz B, et al. Boron–Diindomethene (BDI) Dyes and Their Tetrahydrobicyclo Precursors—en Route to a New Class of Highly Emissive Fluorophores for the Red Spectral Range. *Chem - Eur J*, 2004:10(19):4853-4871.

[42] Miao W, Feng Y, Wu Q, Sheng W, Li M, Liu Q, et al. Phenanthro[b]-Fused BODIPYs through Tandem Suzuki and Oxidative Aromatic Couplings: Synthesis and Photophysical Properties. *J Org Chem*, 2019:84(15):9693-9704.

[43] Zhou Z, Zhou J, Gai L, Yuan A, Shen Z. Naphtho[b]-fused BODIPYs: one pot Suzuki-Miyaura-Knoevenagel synthesis and photophysical properties. *Chem Commun*, 2017:53(49):6621-6624.

[44] Maeda C, Todaka T, Ema T. Carbazole-Based Boron Dipyrromethenes (BODIPYs): Facile Synthesis, Structures, and Fine-Tunable Optical Properties. *Org Lett*, 2015:17(12):3090-3093.

[45] Ni Y, Zeng W, Huang K-W, Wu J. Benzene-fused BODIPYs: synthesis and the impact of fusion mode. *Chem Commun*, 2013:49(12):1217-1219.

[46] Yu C, Fang X, Wu Q, Jiao L, Sun L, Li Z, et al. A Family of BODIPY-like Highly Fluorescent and Unsymmetrical Bis(BF2) Pyrrolyl–Acylhydrazone Chromophores: BOAPY. *Org Lett*, 2020:DOI:

10.1021/acs.orglett.1020c00940.

[47] Wang J, Boens N, Jiao L, Hao E. Aromatic [b]-fused BODIPY dyes as promising near-infrared dyes. *Org Biomol Chem*, 2020:DOI: 10.1039/D1030OB00790K.

[48] Descalzo AB, Xu H-J, Xue Z-L, Hoffmann K, Shen Z, Weller MG, et al. Phenanthrene-Fused Boron−Dipyrromethenes as Bright Long-Wavelength Fluorophores. *Org Lett*, 2008:10(8):1581-1584.

[49] Descalzo AB, Xu H-J, Shen Z, Rurack K. Influence of the meso-substituent on strongly red emitting phenanthrene-fused boron–dipyrromethene (BODIPY) fluorophores with a propeller-like conformation. *J Photoch PhotoBio A*, 2018:352:98-105.

[50] Cui J, Sheng W, Wu Q, Yu C, Hao E, Bobadova-Parvanova P, et al. Synthesis, Structure, and Properties of Near-Infrared [b]Phenanthrene-Fused BF2 Azadipyrromethenes. *Chem - Asian J*, 2017:12(18):2486-2493.

[51] Heyer E, Retailleau P, Ziessel R. α-Fused Dithienyl BODIPYs Synthesized by Oxidative Ring Closure. *Org Lett*, 2014:16(9):2330-2333.

[52] Ito H, Sakai H, Suzuki Y, Kawamata J, Hasobe T. Systematic Control of Structural and Photophysical Properties of π-Extended Mono- and Bis-BODIPY Derivatives. *Chem - Eur J*, 2020:26(1):316-325.

[53] Sun Z-B, Guo M, Zhao C-H. Synthesis and Properties of Benzothieno[b]-Fused BODIPY Dyes. *J Org Chem*, 2016:81(1):229-237.

[54] Yang X, Jiang L, Yang M, Zhang H, Lan J, Zhou F, et al. Pd-Catalyzed Direct C–H Functionalization/Annulation of BODIPYs with Alkynes to Access Unsymmetrical Benzo[b]-Fused BODIPYs: Discovery of Lysosome-Targeted Turn-On Fluorescent Probes. *J Org Chem*, 2018:83(16):9538-9546.

[55] Luo L, Wu D, Li W, Zhang S, Ma Y, Yan S, et al. Regioselective Decarboxylative Direct C–H Arylation of Boron Dipyrromethenes (BODIPYs) at 2,6-Positions: A Facile Access to a Diversity-Oriented BODIPY Library. *Org Lett*, 2014:16(23):6080-6083.

[56] Chen Q, Schollmeyer D, Müllen K, Narita A. Synthesis of Circumpyrene by Alkyne Benzannulation of Brominated Dibenzo[hi,st]ovalene. *J Am Chem Soc*, 2019:141(51):19994-19999.

[57] Lu Y, Qiao Y, Xue H, Zhou G. From Colorless to Near-Infrared S-Heteroarene Isomers: Unexpected Cycloaromatization of Cyclopenta[b]thiopyran Catalyzed by PtCl2. *Org Lett*, 2018:20(21):6632-6635.

[58] Aguilar E, Sanz R, Fernández-Rodríguez MA, García-García P. 1,3-Dien-5-ynes: Versatile Building Blocks for the Synthesis of Carbo- and Heterocycles. *Chem Rev*, 2016:116(14):8256-8311.

[59] Mamane V, Hannen P, Fürstner A. Synthesis of Phenanthrenes and Polycyclic Heteroarenes by Transition-Metal Catalyzed Cycloisomerization Reactions. *Chem - Eur J*, 2004:10(18):4556-4575.

[60] Fürstner A, Mamane V. Flexible Synthesis of Phenanthrenes by a PtCl2-Catalyzed Cycloisomerization Reaction. *J Org Chem*, 2002:67(17):6264-6267.

[61] Zhou J, Wu B, Zhou Z, Tian J, Yuan A. A Novel Naphthalene-Fused Boron Dipyrromethene (BODIPY)-Based Near Infrared Fluorescent Probe for Detecting Fluoride in Living Cells. *Chin J Org Chem*, 2019:39(2):406-411.

[62] Hayashi Y, Yamaguchi S, Cha WY, Kim D, Shinokubo H. Synthesis of Directly Connected

BODIPY Oligomers through Suzuki–Miyaura Coupling. *Org Lett*, 2011:13(12):2992-2995.

[63] Gai L, Mack J, Lu H, Yamada H, Kuzuhara D, Lai G, et al. New 2,6-Distyryl-Substituted BODIPY Isomers: Synthesis, Photophysical Properties, and Theoretical Calculations. *Chem - Eur J*, 2014:20(4):1091-1102.

Captions of Tables, Fig.s and Schemes

Scheme 1. Two possible cycloaromatization pathways for dienylalkyne derivatives.

Scheme 2. Synthetic route to BODIPYs **4a**, **4b**, **4c**, and **5b**.

Fig. 1. ^{1}H NMR superposition of **3b**, **4b**, and **5b** (400 MHz, $CDCl_3$).

Fig. 2. X-ray structures of **3b** and **3c**. Hydrogen atoms were omitted for clarity. The thermal ellipsoids were set at 50% probability.

Fig. 3. UV/Vis absorption (left) and normalized fluorescence (right) spectra of **4a**, **4b**, **4c**, and **5b** in DCM.

Table 1. Spectroscopic and photophysical properties of **3a-5b** in CH_2Cl_2 at 298K.

Fig. 4. DFT calculated frontier molecular orbital profiles and energy levels.

Fig. 5. The overlaid plots of the calculated electronic transition (gray bars) and experimental UV-Vis spectra (colored lines) of **4b** and **5b**. The NICS(0) values (ppm) at the geometric center points of the corresponding five-/six-membered rings.

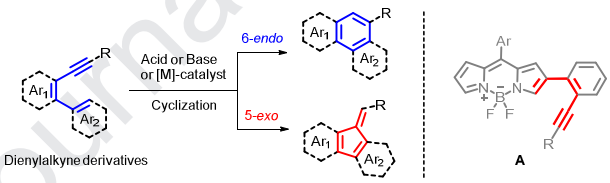

Scheme 1. Two possible cycloaromatization pathways for dienylalkyne derivatives.

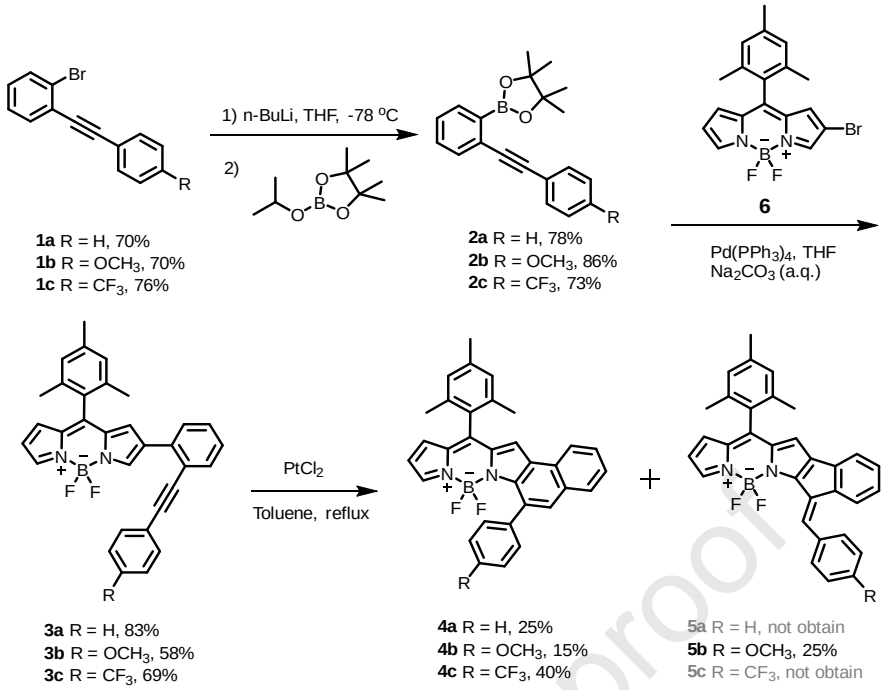

Scheme 2. Synthetic route to BODIPYs **4a**, **4b**, **4c**, and **5b**.

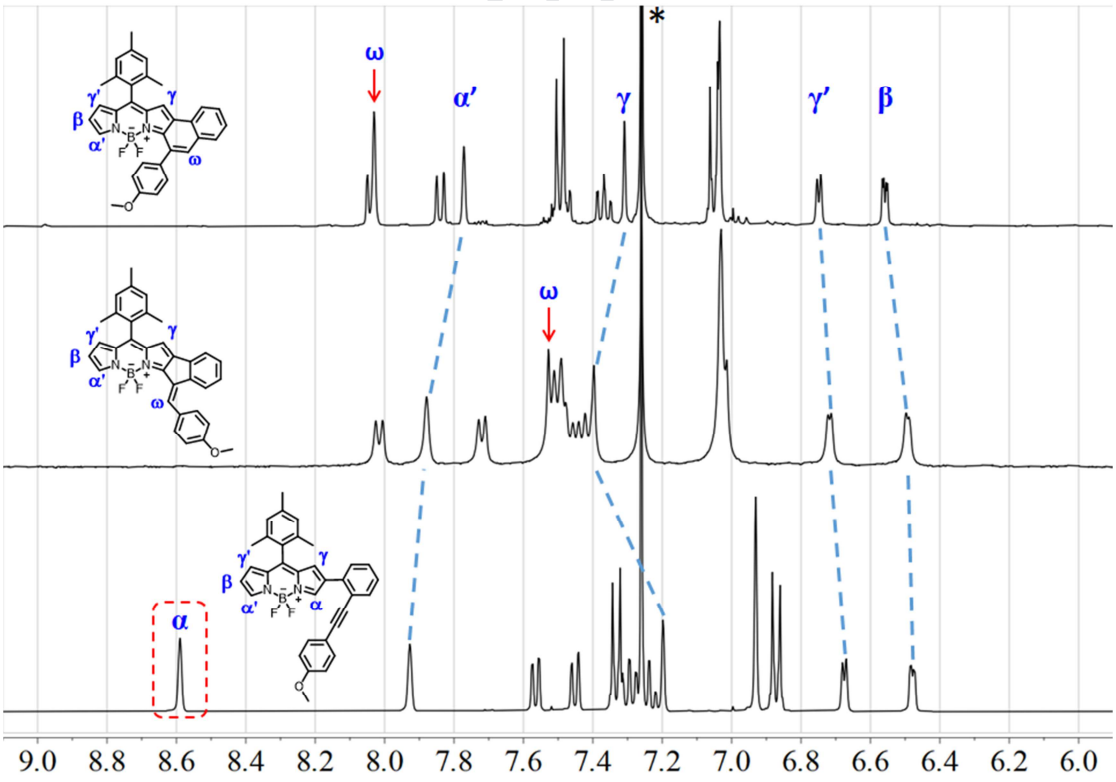

Fig. 1. ^{1}H NMR superposition of **3b**, **4b**, and **5b** (400 MHz, $CDCl_3$).

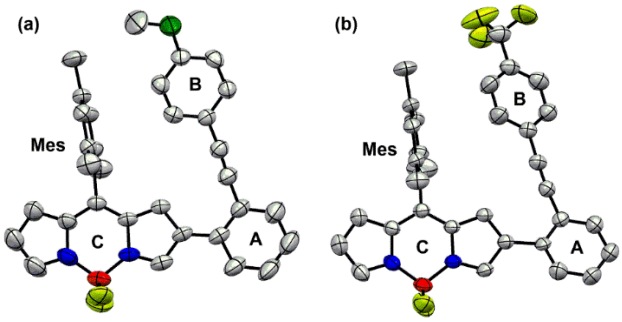

Fig. 2. X-ray structures of **3b** (CCDC No. 2006582) and **3c** (CCDC No. 2006583). Hydrogen atoms were omitted for clarity. The thermal ellipsoids were set at 50% probability. C gray, N blue, F yellowish green, B red, and O deep green.

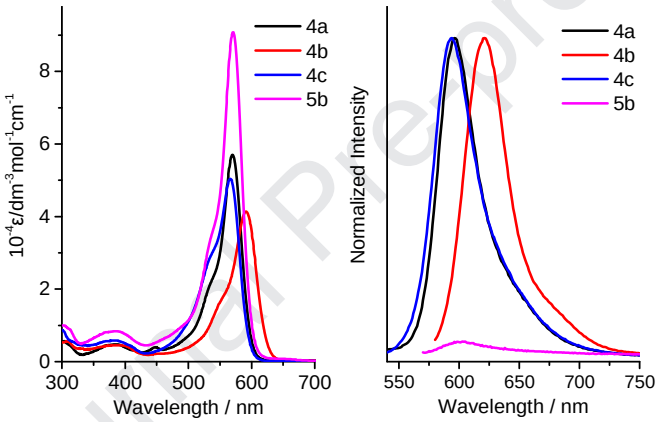

Fig. 3. UV/Vis absorption (left) and normalized fluorescence (right) spectra of **4a**, **4b**, **4c**, and **5b** in DCM. (For **4a** and **4c**, λ_{ex} = 470 nm; for **4b** and **4d**, λ_{ex} = 550 nm. The emission plot of **5b** was not normalized due to low intensity.)

Table 1. Spectroscopic and photophysical properties of **3a-5b** in CH_2Cl_2 at 298K.

	λ_{abs}^{max} [nm]	ε_{abs}[a] [M^{-1} cm^{-1}]	λ_{em}^{max} [nm]	$\Delta\nu_{em-abs}$[b] [cm^{-1}]	Φ_F[c]	τ[d] [ns]	κ_r[e] [10^8 s^{-1}]	κ_{nr}[f] [10^8 s^{-1}]
3a	537	33000	593	1759	0.20	6.27	0.32	1.28
3b	538	28000	599	1893	0.25	3.76	0.66	1.99
3c	536	38300	586	1609	0.20	6.38	0.31	1.25
4a	570	56200	597	793	0.18	3.74	0.48	2.19

4b	591	41000	621	817	0.56	4.78	1.17	0.92
4c	567	50000	594	817	0.19	4.95	0.38	1.64
5b	571	91000	600	846	0.01	—	—	—

[a] Molar absorption coefficients of the maximum absorption peak. [b] Stokes-shift value. [c] The fluorescence quantum yields were calculated using fluorescein as the standard (Φ_F = 0.95 in 0.1 M NaOH) for **3a**, **3b**, and **3c** and Rhodamine 6G as the standard (Φ_F = 0.95 in ethanol) for **4a**, **4b**, **4c**, and **5b**. The standard errors are less than 5%. [d] Fluorescence liftime. [e] The radiative decay rate, $k_r = \Phi_F/\tau$. [f] The nonradiative decay rate, $k_{nr} = (1-\Phi_F)/\tau$.

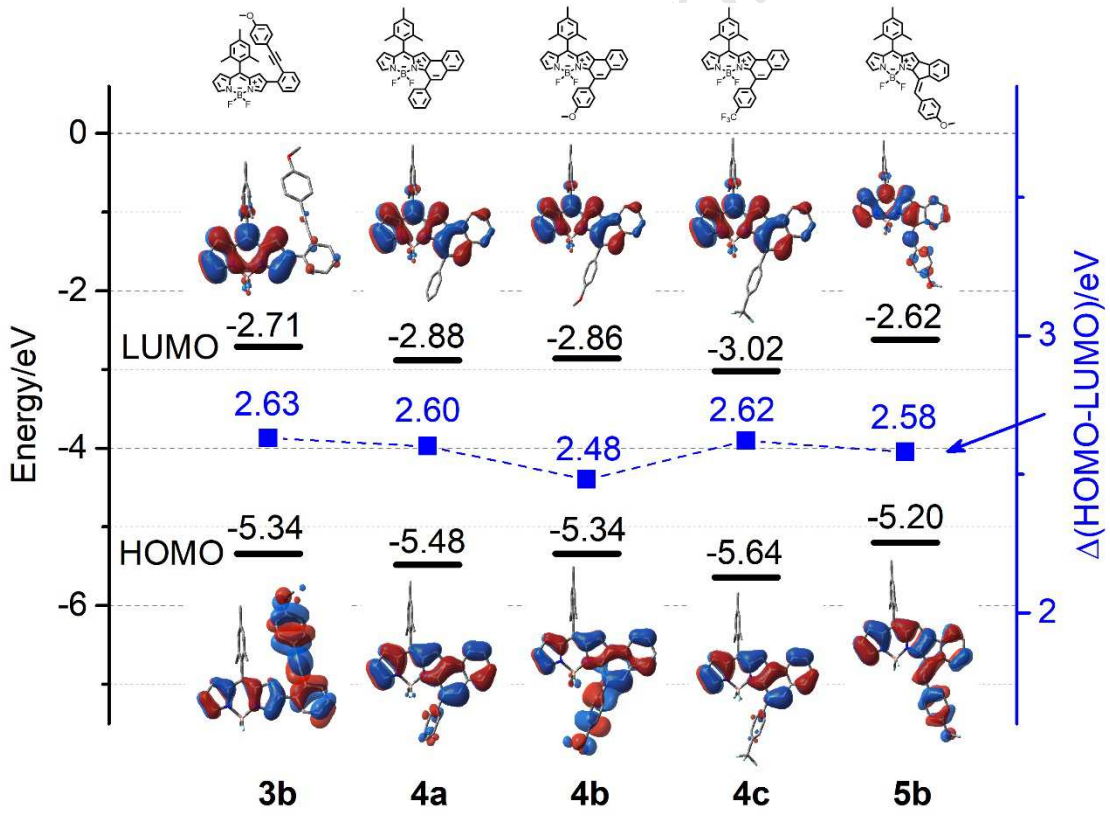

Fig. 4. DFT calculated frontier molecular orbital profiles and energy levels.

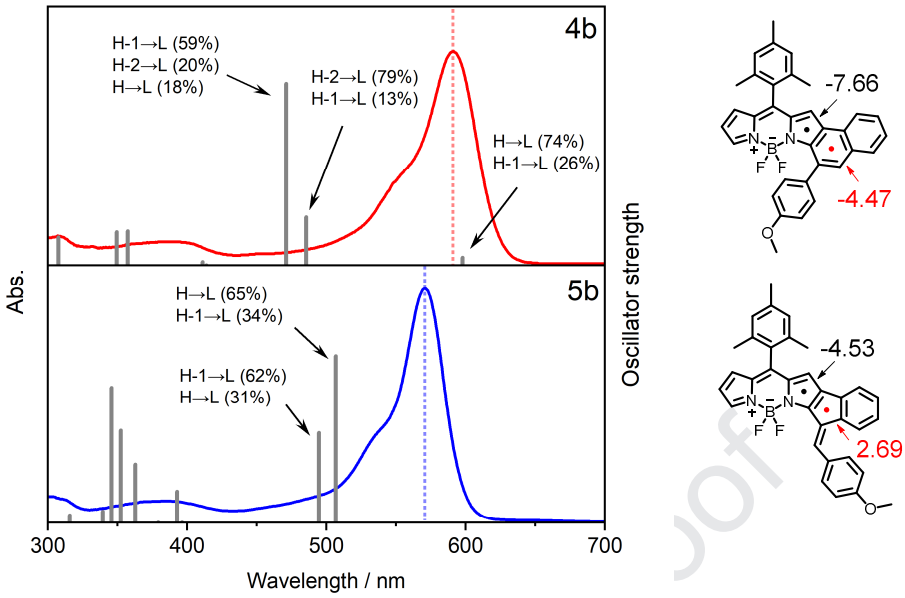

Fig. 5. The overlaid plots of the calculated electronic transition (gray bars) and experimental UV-Vis spectra (colored lines) of **4b** and **5b**. The NICS(0) values (ppm) at the geometric center points of the corresponding five-/six-membered rings.

Highlights

A facile method for aromatic ring [b]-fused BODIPYs was reported

Methoxy group facilitate the formation of two isomers with different photophysical properties in one pot reaction.

Naphtho[*b*]-fused BODIPY exhibits higher quantum yield (0.56 in DCM), while the isomeric indeno[*b*]-fused BODIPY shows stronger absorption intensity.

Theoretical calculations revealed the structure-property relationships of BODIPYs with different conformations.

Declaration of interests

☒ The authors declare that they have no known competing financial interests or personal relationships that could have appeared to influence the work reported in this paper.

☐The authors declare the following financial interests/personal relationships which may be considered as potential competing interests: